DOI 10.1007/s11015-022-01256-8
Metallurgist, Vol. 65, Nos. 9-10, January, 2022 (Russian Original Nos. 9-10, September–October, 2021)

MICROSTRUCTURE AND MECHANICAL PROPERTIES OF TITANIUM ALLOY VT6 AND VT20L DIFFUSION JOINTS

A. Ya. Travyanov,[1] P. V. Petrovsky,[2] V. V. Cheverikin,[3] A. O. Lagutin,[4] M. G. Khomutov,[5] and V. V. Luk'yanov[6]

UDC 620.172.2; 621.7

Joints of VT6 and VT20L titanium alloys are prepared by diffusion welding in an autoclave (at a temperature of 920°C, a pressure of 4 MPa, and holding time of 4 h) and during hot isostatic pressing (at a temperature of 930°C, a pressure of 100 MPa, a holding time of 2 h). Alloy Ti6Al4V components are prepared in two different ways, i.e., by rolling and selective laser melting methods. After welding in an autoclave, defects are found in the microstructure of the specimens in the diffusion joint area. No defects are found within the microstructure of the specimen prepared by hot isostatic pressing. Welded specimens have a high level of strength properties corresponding to the VT20L base alloy material level.

Keywords: VT6 alloy, VT20L alloy, selective laser fusion, diffusion welding, hot isostatic pressing.

Currently within Russia in gas turbine engine building complexly shaped large titanium components are prepared by precision casting followed by machining. The process of casting manufacture is complex, difficult, and includes operations of preparing fittings, investment/ burnt-out molds, melting and casting with melting in a vacuum, finishing and monitoring operations [1–3]. In this case there are certain limitations with respect to geometry of the castings obtained due to the production process possibilities. In addition there is a risk of scrap for especially complex geometry components in the machining stage.

One way of reducing production limitations in the manufacture of especially complex shaped titanium casting, and also repair of "broken" castings during component production is diffusion welding to cast elements grown by a selective laser melting method (SLM). In contrast to direct laser growing of elements on a cast base [4], in this method there are no limitations connected with positioning of a robot and melting head in cast component areas that are difficult to access.

It is well known that by diffusion welding it is possible to prepare titanium components with properties of a welded joint comparable with those of the basic material [5]. As a rule, diffusion welding (DW) of titanium alloys is implemented in an autoclave at an operating temperature of 930°C, pressure of 4 MPa, and holding time for 4 h. In this case there is complete welding of components without defects at the contact boundary [6–8]. It is also well known that with diffusion welding in an autoclave a workpiece with a different grain

[1] National University of Science and Technology MISiS, Moscow, Russia; e-mail: trav@misis.ru.

[2] National University of Science and Technology MISiS, Moscow, Russia; e-mail: pavelpv@inbox.ru.

[3] National University of Science and Technology MISiS, Moscow, Russia; e-mail: cheverikin80@rambler.ru.

[4] National University of Science and Technology MISiS, Moscow, Russia; e-mail: and57769588@yandex.ru.

[5] National University of Science and Technology MISiS, Moscow, Russia; e-mail: khomutov@misis.ru.

[6] Scientific and Production Association Technopark of Aviation Technologies (SPA Technopark AT), Ufa, Russia; e-mail: lukianovv@bk.ru.

Translated from Metallurg, Vol. 65, No. 10, pp. 61–66, October, 2021. Russian DOI 10.52351/00260827_2021_10_61. Original article submitted July 19, 2021.

Table 1
Test Alloy VT20L and VT6 Chemical Composition

Alloy	Ti	Al	V	Mo	Zr
VT6	Base	6	4	–	–
VT20L	Base	6.95	1.88	2.15	2.2

size may retain zones without forming a welded joint [9]. One way of resolving this problem is an increase in pressure during welding.

Results achieved in the field of selective laser welding technology indicate that the properties of titanium alloys obtained by the SLM method are comparable with those of rolled product [10, 11]. In this case for the SLM process there is typically good stamp resolution that makes it possible to prepare especially complex objects including cellular structures that lay the foundations for construction of promising technology [12–14].

A significant improvement in mechanical properties for components prepared bot by casting and selective laser melting is achieved as a result of using hot isostatic compaction (HIP). Within the HIP process due to argon pressure of more than 100 MPa i superplastic condition at temperatures of the order of 900–950°C and with holding of the order of 2 h there is all-round object compression that leads to avoidance of internal defects (cracks and pores) [15–17].

This work is devoted to studying diffusion joining of cast titanium alloy VT20L and alloy VT6 prepared by rolling and SLM using diffusion welding in an autoclave and during the HIP process.

Research Procedure

Workpieces of alloy VT20L were prepared for the study by casting and for alloy VT6 by SLM. The chemical compositions of alloys VT20L and VT6 are provided in Table 1.

Cast workpiece preparation was accomplished in a vacuum melting and casting unit with a floating electrode and pouring into a centrifugally rotating ceramic mold.

The SLM process was accomplished in a SLM-280 unit from alloy VT6 (Ti6Al4V) powder fraction 5–45 μm, prepared by gas atomization with a powerful laser radiation regime with 240 W, and laser beam scanning rate 1060 mm/sec.

All specimens before diffusion welding were subjected to the HIP operation by a regime: temperature 930 ± 5°C, holding time 2 h, and argon pressure 100 MPa.

During specimen preparation for diffusion welding there was encapsulation and evacuation of the joint zone. Encapsulation was accomplished by heating over the workpiece joint contour obtained by rolling and additive growth, followed by welding pipes for evacuation of the joint zone.

Specimen preparation for diffusion welding included the following stages: machining a flat surface, activation of the surface by chemical etching, assembly by welding argon-arc of two workpieces in order to provide sealing of the diffusion joint zone, and evacuation of the joint zone.

Diffusion welding was accomplished in an autoclave by a regime: temperature 930 ± 5°C, holding time 4 h, argon pressure 4 MPa; in a gas chamber by a regime: temperature 930 ± 5°C, holding time 2 h, argon pressure 100 MPa. Labeling and regimes for test specimens preparation of material pairs are provided in Table 2.

Table 2
Test Alloy Preparation Regimes

Alloy specimen grade	Material pair description	DW type	Regime
VT20L-VT6	VT20L – workpiece prepared by casting with subsequent HIP treatment; VT6 – workpiece cut from hot-rolled plate 32 mm thick	Diffusion welding in autoclave	Temperature: 930 ± 5°C; Holding time – 4 h; Argon pressure – 4 MPa
VT20L-VT6 (HIP)	VT20L – workpiece prepared by casting with subsequent HIP treatment; VT6 – workpiece cut from hot-rolled plate 32 mm thick	Diffusion welding in a gasostat	Temperature: 930 ± 5°C; Holding time – 2 h; Argon pressure – 100 MPa
VT20L-SLM	VT20L – workpiece prepared by casting with subsequent HIP treatment; SLM – workpiece prepared from VT6 powder by method of selective laser melting followed by HIP treatment	Diffusion welding in autoclave	Temperature: 930 ± 5°C; Holding time – 4 h; Argon pressure – 4 MPa
VT20L-SLM (HIP)	VT20L – workpiece prepared by casting with subsequent HIP treatment; SLM – workpiece prepared from VT6 powder by method of selective laser melting followed by HIP treatment	Diffusion welding in a gasostat	Temperature: 930 ± 5°C; Holding time – 2 h; Argon pressure – 100 MPa

Specimen microstructure and fractograms were studied using a (SEM) TESCAN VEGA LMH (Tescan, Czech Republic) scanning electron microscope with an LaB_6 cathode and an Oxford Instruments Advanced AZtecEnergy X-ray energy dispersion system.

Welded joint mechanical properties by a standard test ,method in uniaxial tension according to GOST 1497–84 on cylindrical specimens type II (No. 7). Prepared standard specimens were tensile tested at room temperature and 300°C in a Zwick/Roell Z250 (Zwick GmbH & Co., Germany) universal test machine.

Impact bend testing was conducted according to GOST 9454-78 using a SI-1M (Instron, USA) pendulum impact machine with a U shape concentrator.

Three point bend testing was conducted according to GOST 14019-2003 in an LF100 (Walter+Bay AG, Switzerland) servo-hydraulic universal test machine. Test were conducted on flat specimens of rectangular section (width 100 mm, thickness 2 mm) up to development of the first crack with measurement of the bending angle. Loading rate 4 mm/min.

The specimen cutting regime for mechanical tests of welded ingots is shown in Fig. 1.

Research Results and Discussion

It is well known that according to titanium alloy classification with respect to structure in an annealed condition alloy VT20L relates to the pseudo-α alloy class (phase composition: 94 vol.% α-phase and 6 vol.%

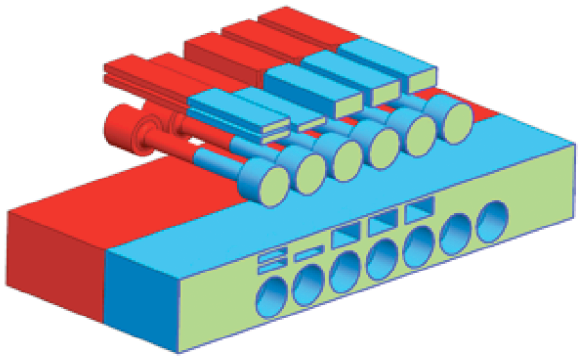

Fig. 1. Layout of specimen cut-outs from welded ingots of different material pairs.

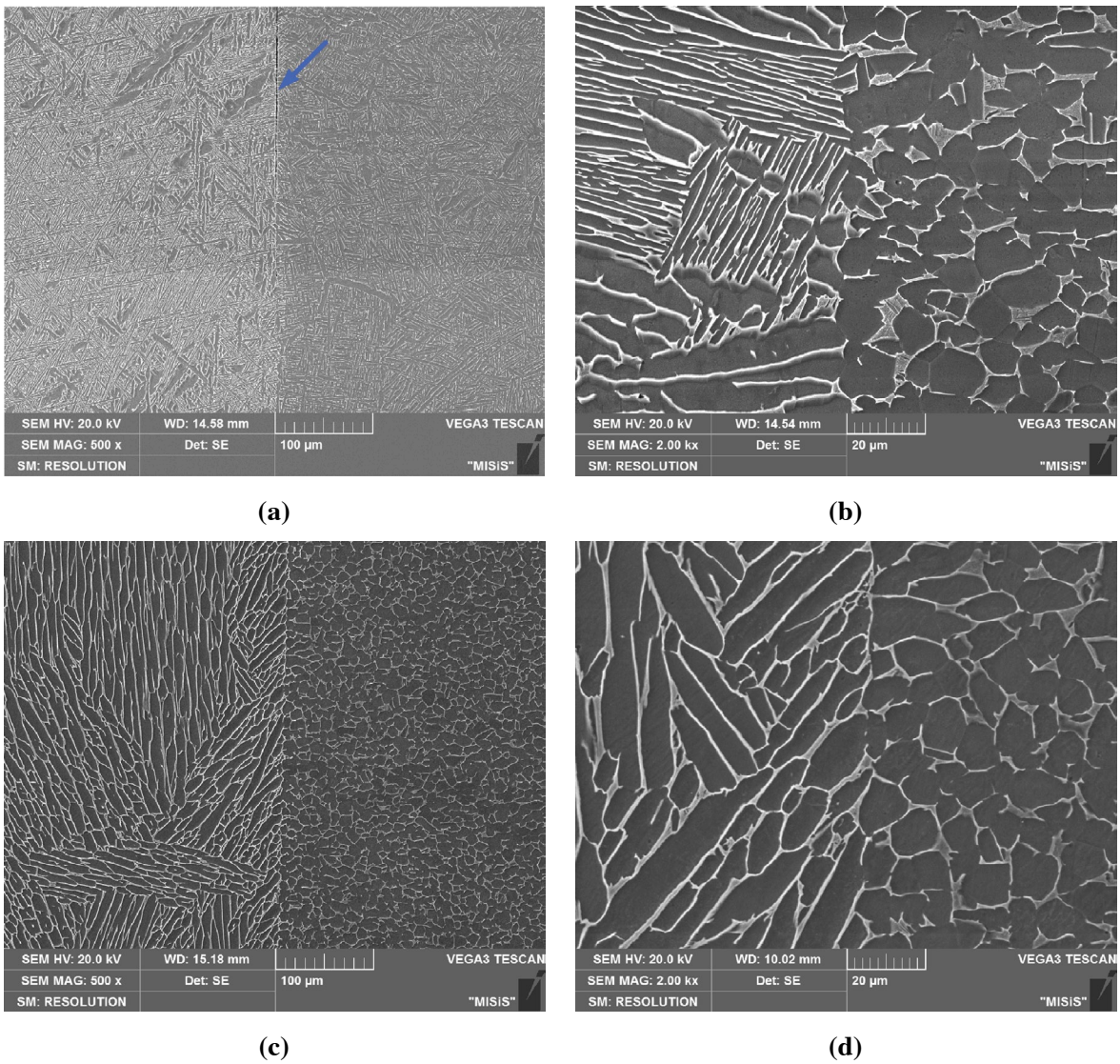

Fig. 2. Microstructure of welded joint specimens of a pair of materials VT20L-VT6 (a, b) and VT20L-VT6 (HIP) (c, d) after diffusion welding VT20L part to the left, VT6 to the right after rolling) at different magnifications (SEM): (a, c) magnification × 200; (b, d) magnification × 2000.

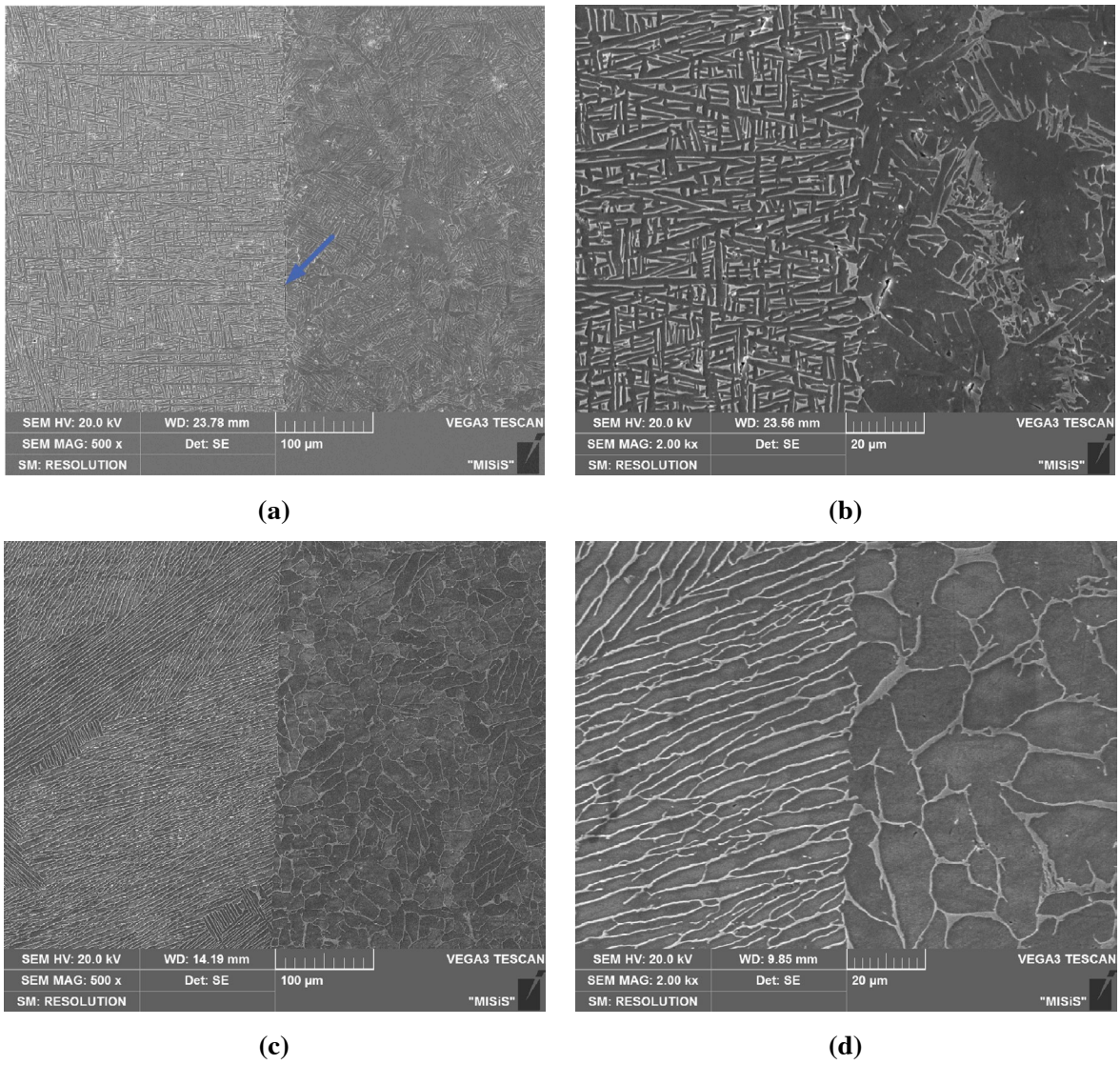

Fig. 3. Welded joint specimen microstructure for pair of materials VT20L-SLM (a, b) and VT20L-SLM (HIP) (c, d) after diffusion welding (VT20L part to the left, VT6 after HIP to the right) at different magnifications: (a, c) magnification × 200; (b, d) magnification × 2000.

β-phase), and alloy VT-6 corresponds to α + β-class with phase composition: 88 vol.% α-phase, 12 vol.% β-phase [18]. The test specimen microstructure in the region of a welded joint is given in Figs. 2 and 3. For all test material pairs prepared in an autoclave presence of defects is observed, i.e., microcracks and unwelded areas shown by arrows in Figs. 2a and 3b that confirm the nonuniform joining of metals during holding in an autoclave at low pressure of 4 MPa. Similar defects were not observed in specimens welded during the HIP process (Figs. 2c and 3c). In all of the microstructure images for each of the materials there is typically presence of α- (dark phase in Figs. 2 and 3) and β-phase (light phase in Figs. 2 and 3). The microstructure of half of the welded joints of alloy VT20L is not uniform. It consists of both coarse α-phase grains of lamellar structure surrounded by a β-phase network, and also of fine α- and β-phases of lamellar structure. Half of the welded specimens in the alloy VT6 region were prepared by rolling (Fig. 2), the microstructure has predominantly equiaxed spherical α-phase grains with layers of β-phase over boundaries, and also coarse lamellar colonies of

Table 3
Tensile Test Results

Specimen designation	T_{room}				300°C		
	E, GPa	$\sigma_{0.2}$, MPa	σ_u, MPa	δ, %	$\sigma_{0.2}$, MPa	σ_u, MPa	δ, %
VT20L-VT6	136 ± 8	863 ± 35	867 ± 36	2.8 ± 1.5	478 ± 13	560 ± 23	6.0 ± 3.9
VT20L-VT6 (HIP)	130 ± 3	860 ± 26	877 ± 19	2.6 ± 0.6	483 ± 12	584 ± 56	8.6 ± 1.4
VT20L-SLM	128 ± 2	840 ± 6	863 ± 9	2.2 ± 1.7	453 ± 2	580 ± 12	8.2 ± 1.6
VT20L-VT6 (HIP)	133 ± 3	825 ± 7	860 ± 17	4.2 ± 1.3	445 ± 20	575 ± 20	9.5 ± 1.6
VT20L	127 ± 6	800 ± 18	830 ± 30	6.8 ± 1.7	–	–	–

Table 4
Test Results in Three-Point Bending and Impact Bending

Specimen designation	$\sigma_{0.2}$, MPa	σ_u, MPa	Bending angle α, deg	Impact strength KCU, kJ/cm^2
VT20L-VT6	1530 ± 30	2100 ± 70	33 ± 15	45 ± 10
VT20L-VT6 (HIP)	1570 ± 40	2150 ± 90	29 ± 6	62 ± 2
VT20L-SLM	1610 ± 35	2170 ± 50	25 ± 4	49 ± 18
VT20L-SLM (HIP)	1510 ± 70	2010 ± 130	24 ± 2	64 ± 5

dispersed $\alpha+\beta$-phases. A similar microstructure may be observed in half of the welded specimens of alloy VT6 prepared by the SLM method (Fig. 3) with one difference: coarse grains of α-phase have a predominantly lamellar structure.

Test specimen mechanical properties are provided in Tables 3 and 4. After welding during the HIP process the level of strength properties in tensile tests (Young's modulus E, yield strength σ_y, ultimate strength σ_u) are somewhat lower than for similar welded pairs of materials prepared in an autoclave. However, in view of presence of areas of defects of a welded joint for specimens prepared in an autoclave, relative elongation δ, bending angle α, and impact strength KCU often have a more reduced value and greater scatter of the confidence range. Properties are provided for comparison in Table 3 for tension at room temperature of the basic alloy VT20L material. It is seen that all welded specimens exhibit a higher level of strength properties but low ductility indices δ.

Fractograms of specimens fractures after tension at room temperature are provided in Figs. 4 and 5. The fractures of specimens undergoing diffusion welding in an autoclave (Fig. 4a, b) and by the HIP regime (see Fig. 5a, b)

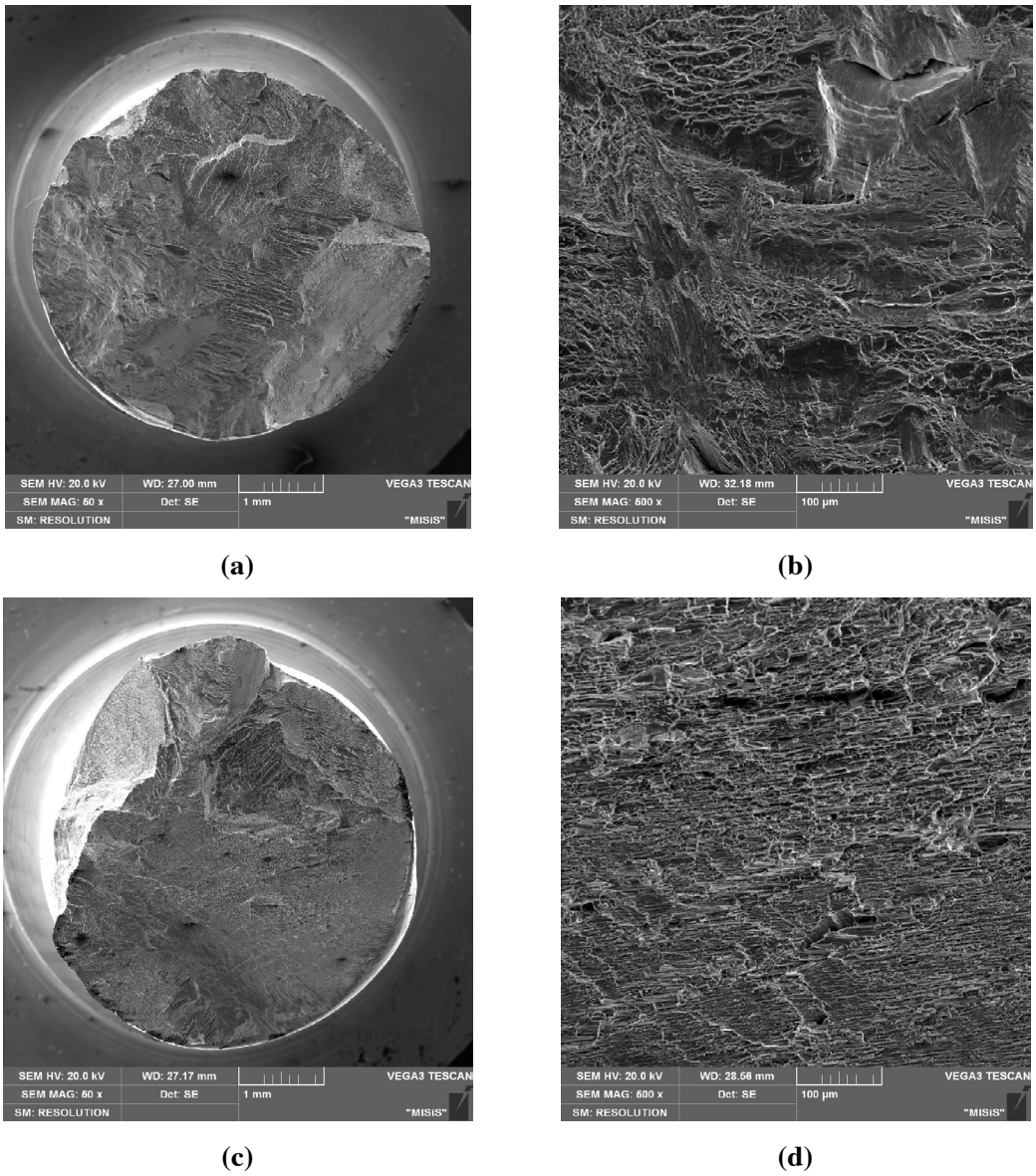

Fig. 4. Specimen fracture fractograms for pair of materials VT20L-VT6 (a, b) and VT20L-VT6 (HIP) (c, d) after tensile testing at room temperature at different magnifications (SEM): (a, c) magnification × 50; (b, d) magnification × 500.

have a predominantly pitted structure with a minimum amount of brittle component that points to the predominantly ductile nature of failure.

On the whole the welded VT6 specimens obtained produced by different technology and with a different grain structure exhibit a high level of mechanical properties satisfying the specifications of standard documentation for hot-rolled annealed plates of ally VT6. No welded joint defects were observed.

Conclusion. The possibility has been demonstrated of preparing defect-free objects by diffusion welding during hot isostatic compaction of different pairs of alloys VT20L and VT6 materials (prepared by rolling and selective laser melting) exhibiting different phase compositions of the morphology and structural components. Welded specimens exhibit a level of strength properties corresponding to that of the basic VT20L material.

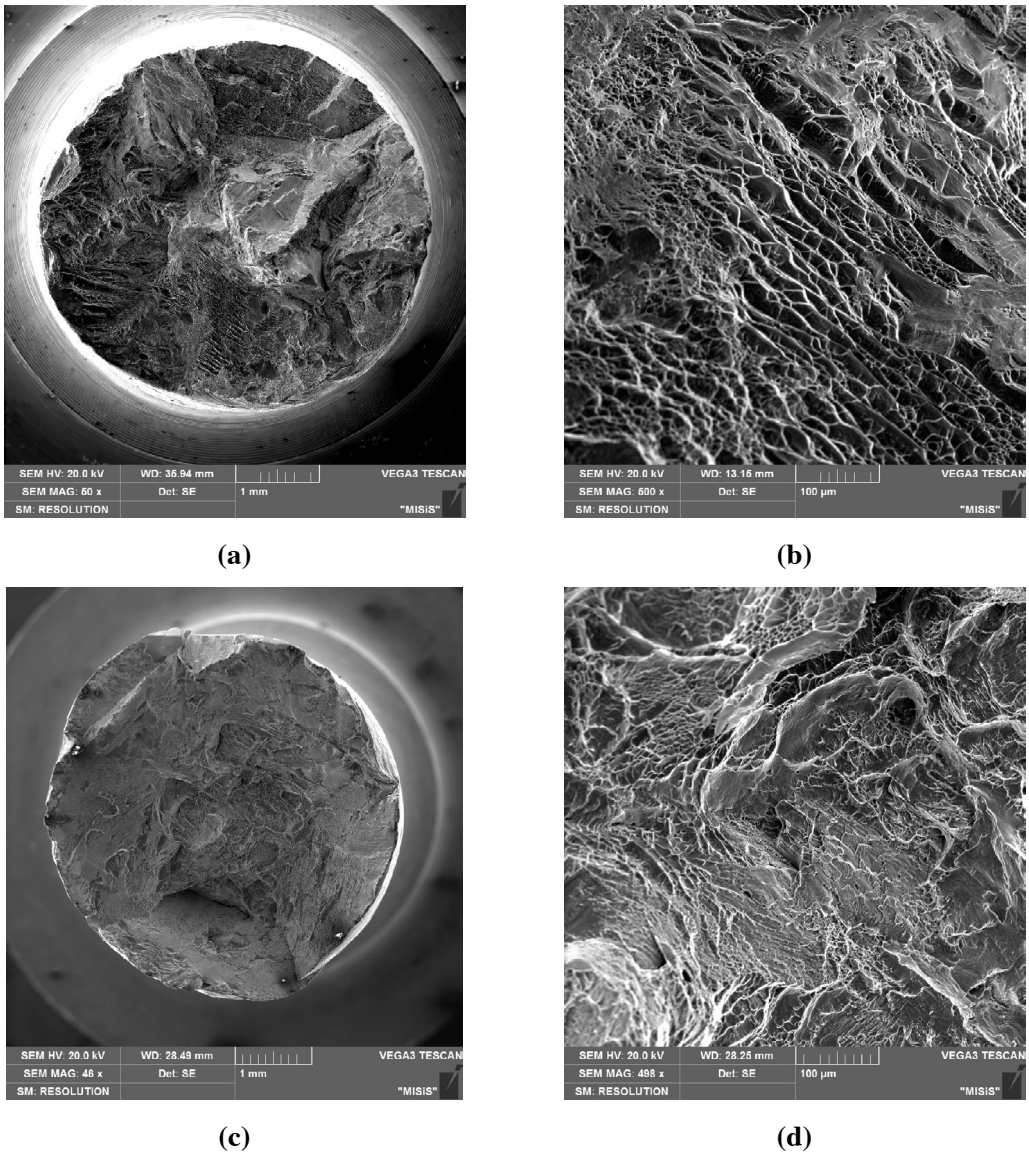

Fig. 5. Specimen fracture fractograms for pair of materials VT20L-SLM (a, b) and VT20L-SLM (HIP) (c, d) after tensile testing at room temperature at different magnifications (SEM): (a, c) magnification × 50; (b, d) magnification × 500.

Work was carried out with financial support of the Russian Federation Ministry of Science and Higher Education within the framework of Government declaration No. 218 for agreement of supply of a subsidy No. 075-11-2019-058 of 11.25.2019 "Creation of production of locally reinforced titanium alloy components operating under high loading and temperature conditions for prospective aircraft gas turbine engines."

REFERENCES

1. A. Yu. Demenok, A. A. Ganneev, O. B. Demenok, et al., "Development of resource saving technology for preparing large titanium alloy castings," *Vestn. YuUrGU Ser. Metallurgiya,* **15**, No. 2, 20–25 (2015).
2. A. V. Koltyrgin, V. E. Bazhenov, and A. V. Fadeev, "Improvement of casting technology for large aircraft engine components of all VT20L using computer modeling methods," *Tsvet. Met.,* No. 5, 8085 (2015).

3. V. D. Belov, A. V. Fadeev, S. p. Pavlinich, et al., "Effect of material form on the quality of titanium alloy castings," *Liteishchik Rossii,* No. 3, 19–26 (2015).
4. A. Ya. Travyanov, P. V. Petrovskii, G. A. Turichin, et al., "Preparation of complex shape hybrid elements of aircraft engines by a combination of casting and direct laser growing technology. Additive technology in Russian industry," in: *Proc. Sci.-Pract. Conf. 10 February 2015,* Vol. 1, GGUP VIAM, Moscow (2015), pp. 1–10.
5. R. V. Safiullin, M. Kh. Mukhametrakhimov, A. R. Safiullin, et al., "The study of technological properties of the titanium alloy Ti–6Al–4V. Part 2," *Lett. Mater.,* **8**, No. 3, 329–334 (2018).
6. H. S. Lee, J. H. Yoon, and Y. M. Yi, "Solid state diffusion bonding of titanium alloys," *Solid State Phenom. Trans Tech Publications, Ltd.,* **124–126**, 1429–1432 (2007).
7. K. Chandrappa, C. S. Sumukha, B. B. Sankarsh, et al., "Superplastic forming with diffusion bonding of titanium alloys," *Materials Today: Proc. Elsevier Ltd.,* **27**, 2909–2913 (2019).
8. E. Yakushina, A. Reshetov, I. Semenova, et al., "The influence of the microstructure morphology of two phase Ti– 6Al–4V alloy on the mechanical properties of diffusion bonded joints," *Mater. Sci. Eng. A. Elsevier Ltd.,* **726**, 251–258 (2018).
9. É. S. Karakozov, L. M. Orlova, V. V. Peshkov, and V. N. Grigor'evskii, *Titanium Diffusion Welding* [in Russian], Metallurg (1977).
10. M. T. Tsai, Y. W. Chen, C. Y. Chao, et al., "Heat-treatment effects on mechanical properties and microstructure evolution of Ti-6Al-4V alloy fabricated by laser powder bed fusion," *J. Alloys Compd. Elsevier,* **816**, 152615 (2020).
11. S. Murchio, M. Dallago, F. Zanini, et al., "Additively manufactured Ti–6Al–4V thin struts via laser powder bed fusion: Effect of building orientation on geometrical accuracy and mechanical properties," *J. Mech. Behav. Biomed. Mater. Elsevier,* **119**, 104495 (2021).
12. A. Cutolo, B. Engelen, W. Desmet, et al., "Mechanical properties of diamond lattice Ti–6Al–4V structures produced by laser powder bed fusion: On the effect of the load direction," *J. Mech. Behav. Biomed. Mater. Elsevier,* **104**, 103656 (2020).
13. A. Du Plessis, I. Yadroitsava, and I. Yadroitsev, "Ti–6Al–4V lightweight lattice structures manufactured by laser powder bed fusion for load-bearing applications," *Opt. Laser Technol. Elsevier,* **108**, 521–528 (2018).
14. M. Dallago, S. Raghavendra, V. Luchin, et al., "The role of node fillet, unit-cell size and strut orientation on the fatigue strength of Ti–6Al–4V lattice materials additively manufactured via laser powder bed fusion," *Int. J. Fatigue. Elsevier,* **142**, 105946 (2021).
15. J. Benzing, N. Hrabe, T. Quinn, et al., "Hot isostatic pressing (HIP) to achieve isotropic microstructure and retain as built strength in an additive manufacturing titanium alloy (Ti– 6Al–4V)," *Mater. Lett. North-Holland,* **257**, 126690 (2019).
16. D. Herzog, K. Bartsch, and B. Bossen, "Productivity optimization of laser powder bed fusion by hot isostatic pressing," *Addit. Manuf. Elsevier,* **36**, 101494 (2020).
17. P. Li, D. H. Warner, J. W. Pegues, et al., "Investigation of the mechanisms by which hot isostatic pressing improves the fatigue performance of powder bed fused Ti–6Al–4V," *Int. J. Fatigue. Elsevier,* **120**, 342–352 (2019).
18. P. V. Panin, et al., *Practical Handbook for Metallography of Alloys Based on Titanium and its Intermetallics: Textbook* [in Russian], VIAM, Moscow (2020).